Effects of heterogeneity distribution on hillslope stability during rainfalls

Jing-sen Cai [a], E-chuan Yan [a], Tian-chyi Jim Yeh [b],*, Yuan-yuan Zha [b]

[a] *Faculty of Engineering, China University of Geosciences, Wuhan 430074, China*
[b] *Department of Hydrology and Water Resources, University of Arizona, Tucson, AZ 85721, USA*

Abstract

The objective of this study was to investigate the spatial relationship between the most likely distribution of saturated hydraulic conductivity (K_s) and the observed pressure head (P) distribution within a hillslope. The cross-correlation analysis method was used to investigate the effects of the variance of $\ln K_s$, spatial structure anisotropy of $\ln K_s$, and vertical infiltration flux (q) on P at some selected locations within the hillslope. The cross-correlation analysis shows that, in the unsaturated region with a uniform flux boundary, the dominant correlation between P and K_s is negative and mainly occurs around the observation location of P. A relatively high P value is located in a relatively low K_s zone, while a relatively low P value is located in a relatively high K_s zone. Generally speaking, P is positively correlated with q/K_s at the same location in the unsaturated region. In the saturated region, the spatial distribution of K_s can significantly affect the position and shape of the phreatic surface. We therefore conclude that heterogeneity can cause some parts of the hillslope to be sensitive to external hydraulic stimuli (e.g., rainfall and reservoir level change), and other parts of the hillslope to be insensitive. This is crucial to explaining why slopes with similar geometries would show different responses to the same hydraulic stimuli, which is significant to hillslope stability analysis.
© 2016 Hohai University. Production and hosting by Elsevier B.V. This is an open access article under the CC BY-NC-ND license (http://creativecommons.org/licenses/by-nc-nd/4.0/).

Keywords: Cross-correlation analysis; Heterogeneity; Hillslope stability; Saturated hydraulic conductivity; Stochastic conceptualization; Pore-water pressure

1. Introduction

Spatial variability of hydraulic properties of geologic media (e.g., the presence of macropores, fractures, folds, fissures, layers, preferential flow paths, and clay lenses) is the rule rather than the exception. Even seemingly uniform field sites show a high degree of spatial variation in the saturated hydraulic conductivity value (Nielsen et al., 1973). Such variability controls hillslope soil strength distribution,

groundwater flow, pore-water pressure distribution, and seepage force, and, in turn, plays a salient role in hillslope stability along with other factors such as spatial and temporal variability of precipitation. As such, this information allows determination of stress distribution within a hillslope, and appropriate actions can be taken to mitigate possible failure of the hillslope. While the importance of the spatial variability or heterogeneity is well known, it is practically impossible to describe these heterogeneities in detail. In order to overcome this difficulty, probabilistic methods, or methods based on random or stochastic field theory, have been employed in hydrogeology and geotechnical engineering (Yeh, 1992; Gelhar, 1993; Griffiths and Fenton, 1993, 2004; Gui et al., 2000; Srivastava et al., 2010; Cho, 2012; Zhu et al., 2013; Yeh et al., 2015). For example, the random finite element method (RFEM), proposed by Griffiths and Fenton (1993) and Fenton and Griffiths (1993), has been widely used to consider the spatial fluctuations of a parameter

* Corresponding author.

E-mail address: yeh@hwr.arizona.edu (Tian-chyi Jim Yeh).

Peer review under responsibility of Hohai University.

in hillslope stability analysis (Gui et al., 2000; Cho, 2012, 2014; Zhu et al., 2013).

Generally, for a given hillslope, one may collect soil samples at some locations to determine spatial statistics of hydraulic parameters; these spatial statistics are then used to infer the spatial variability of hydraulic parameters across and throughout the hillslope. From the given spatial statistics of the parameters, one can generate many possible spatial distributions of the parameters of the hillslope. Of these distributions, some are favorable to slope stability, and some are not for given rainfall events. In practice, it is rather costly and difficult to characterize the hydraulic heterogeneity by taking soil samples; on the other hand, it is relatively inexpensive and typical to observe hydraulic responses/states, such as the pore-water pressure at hillslope toes or the position of phreatic surface at some locations. As a matter of fact, pore-water pressure distributions are one of the major stresses that control the hillslope stability. This simple reality thus compels us to ask, what can be inferred about the likely spatial distribution of saturated hydraulic conductivity within a hillslope from some observed hydraulic responses or pore-water pressures at some locations within the hillslope?

Zhu et al. (2013) carried out a probabilistic infiltration analysis considering a spatially varying permeability function within a two-dimensional (2D) hillslope. With one set of given statistical parameters, they showed the spatial distributions of saturated hydraulic conductivity that can lead to the highest and lowest groundwater tables in the hillslope. However, they did not focus on the effects of the spatial distribution of saturated hydraulic conductivity in various hydraulic scenarios, nor did they investigate the relationship between the likely distribution of saturated hydraulic conductivity and observed pore-water pressures at some given locations within a hillslope.

Cross-correlation analysis can serve as a quantitative tool for answering the question posed above. Cross-correlation analysis has been widely used by hydrogeologists over the past decade. For example, Yeh et al. (2014) used a simple example to elucidate the cross-correlation relationship between the observed heads in a saturated aquifer and the hydraulic conductivity in a one-dimensional aquifer. Mao et al. (2011) conducted cross-correlation analysis to investigate how the spatial variability of hydraulic parameters, such as the saturated hydraulic conductivity, specific storage, and saturated moisture content, at different locations in unconfined aquifers affect the head at a given location in the unsaturated and saturated regions. Wu et al. (2005) and Sun et al. (2013) used cross-correlation analysis to study the spatial and temporal evolution of cross-correlations between soil properties (transmissivity and storage coefficients) and the head responses at an observation well during a pumping test, in both homogeneous and heterogeneous aquifers.

At present, few have attempted to study the ways in which the saturated hydraulic conductivity at different locations within a hillslope influences the pore-water pressure at some crucial locations within the hillslope. More importantly, few

studies have quantified the relationship between the most likely distribution of saturated hydraulic conductivity and the observed pressure head distribution within a hillslope subject to rainfalls or other external events. This relationship may allow us to better control the pore-water pressure distribution within a hillslope.

The objectives of this study were therefore (1) to examine how the pressure head at a crucial location (e.g., the slope toe) is affected by the saturated hydraulic conductivity at different locations within a hypothetical hillslope; (2) to investigate the relationship between the most likely distribution of saturated hydraulic conductivity and the observed pressure head distribution within a hillslope; and (3) to elucidate the likely distribution of saturated hydraulic conductivity and the flow field distribution within a heterogeneous hillslope subject to some given hydraulic events, which are critical to the study of hillslope stability.

2. Methodology

2.1. Governing equation

While transient flow is more realistic, for the sake of simplicity and a first cut analysis, in this paper we focus on steady-state flow in a heterogeneous hillslope, which is pertinent to long-term status analyses. Here, we assume that the flow in a heterogeneous 2D vertical hillslope cross-section can be described by the following equation:

$$\frac{\partial}{\partial x}\left[K(P)\frac{\partial P}{\partial x}\right] + \frac{\partial}{\partial z}\left[K(P)\frac{\partial (P+z)}{\partial z}\right] = 0 \qquad (1)$$

and is subject to the following boundary conditions:

$$\begin{cases} P(x,z)|_{\Gamma_D} = P_D \\ \left. K(P)\frac{\partial P}{\partial x}n_x + K(P)\left(\frac{\partial P}{\partial z}+1\right)n_z \right|_{\Gamma_N} = q_N \end{cases} \qquad (2)$$

where P is the pressure head; z is the elevation head; $K(P)$ is the hydraulic conductivity-pressure constitutive function; P_D is the prescribed pressure head at the Dirichlet boundary Γ_D; q_N is the specific flux at the Neumann boundary Γ_N; and n_x and n_z are the components of the unit vector $\boldsymbol{n}$ in the x and z directions, respectively, and $\boldsymbol{n}$ is normal to the boundary Γ_N.

2.2. Moisture retention and hydraulic conductivity functions

In order to simulate flow in a hillslope using Eqs. (1) and (2), the moisture retention and hydraulic conductivity curves developed by van Genuchten (1980) and Mualem (1976), respectively, also known as the MVG model, are adopted here, and can be expressed as

$$K(P) = \begin{cases} K_s\{1 - (\alpha|P|)^{n-1}[1 + (\alpha|P|)^n]^{-m}\}^2[1 + (\alpha|P|)^n]^{-m/2} & P < 0 \\ K_s & P \geq 0 \end{cases} \tag{3}$$

$$\theta(P) = \begin{cases} (\theta_s - \theta_r)[1 + (\alpha|P|)^n]^{-m} + \theta_r & P < 0 \\ \theta_s & P \geq 0 \end{cases} \tag{4}$$

where α, n, and m are soil parameters, and $m = 1 - 1/n$; $\theta(P)$ is the volumetric water content; θ_s and θ_r denote the saturated and residual moisture contents, respectively; and K_s is the saturated hydraulic conductivity.

2.3. Random field theory

2.3.1. Stochastic conceptualization of heterogeneity

Hydraulic properties generally exhibit a high degree of spatial variability at various scales (Nielsen et al., 1973; Bouwer, 1978; Yeh, 1992; Cho, 2012). As a result, accurate analysis of flow or stability analysis of a hillslope would require detailed characterization of the hillslope. Nevertheless, it is impossible to sample and map hydraulic properties at every location within a hillslope. We therefore have to estimate or guess their values at a location if there is no measurement of the property (for example, K_s) or if its measurement involves error. Our guess or estimate inevitably causes us to unknowingly conceptualize K_s at the location as a random variable, characterized by a probability distribution. While the probabilistic conceptualization of K_s is rational, the fact is that K_s at a given location, even if it has been determined exactly, can always be treated as a random variable. This is tantamount to stating that the value of K_s determined at that location represents just one of the many possible values of K_s of geologic materials that may have been deposited at this location when the environment comes into existence. Therefore, a hydraulic property of a geologic formation at a given location can always be considered a random variable regardless of whether the property is known or whether it involves measurement error. As a consequence, the hydraulic conductivity field within a hillslope can be considered a collection of random variables. This collection of an infinite number of random variables is then called a stochastic process, or random field. A more detailed introduction of stochastic conceptualization of heterogeneity is provided in Yeh et al. (2015).

Following the procedure of Yeh et al. (2015), in order to describe K_s heterogeneity within a hillslope as a random field, we implicitly assume that the random field has a joint lognormal distribution, which is characterized by a mean (μ_{K_s}), a variance ($\sigma_{K_s}^2$), and a correlation structure described by a covariance function with some correlation scales (λ). Furthermore, we let the natural logarithm of saturated hydraulic conductivity, $\ln K_s$, be F; it has a mean $\overline{F}$ and perturbation, f, whose variance is denoted by σ_f^2. Furthermore, F is assumed to have a statistically isotropic or anisotropic covariance, which is described by an exponential covariance function:

$$R(A, A') = \sigma_f^2 \exp\left[-\sqrt{\frac{(x-x')^2}{\lambda_x^2} + \frac{(z-z')^2}{\lambda_z^2}}\right] \tag{5}$$

where $R(A, A')$ is the autocovariance function of F at points A and A', located at (x, z) and (x', z'), respectively; and λ_x and λ_z are the correlation scales in the x and z directions, respectively.

The autocovariance function of F is a statistical measure of the spatial structure (or spatial pattern) of F heterogeneity. That is, it describes how the value of F at one location is related to the F values at other locations. Physically, the correlation scales of F then represent the average dimensions (e.g., length and thickness) of heterogeneity (e.g., layers or stratifications).

Although other parameters such as α, n, θ_s, and θ_r of the MVG model (Eqs. (3) and (4)) do exhibit spatial variability (Yeh et al., 2015), in this analysis, we assumed that their spatial variability had insignificant effects on hillslope stability issues and they were assumed to be constant throughout the hillslope (Gui et al., 2000; Mao et al., 2011; Cho, 2012, 2014; Zhu et al., 2013).

2.3.2. Random field generation using fast Fourier transformation

In order to generate a random field, a fast Fourier transform code modified from Gutjahr (1989) is used, which is computationally efficient (Zhu et al., 2013) and can produce a reasonable and discretized random field with a defined mean and variance, as well as correlation scales. The random field is represented in the form of discretization, in which the hydraulic conductivity in the random field is generated at each element for finite element analysis. Each realization of the random field is first generated in a rectangular domain, with the same width and height as the hillslope, and then the region outside the boundary of the hillslope is truncated. Thus, a realization with the geometry of the hillslope is generated, following the approach of Zhu et al. (2013).

2.4. Cross-correlation analysis

Cross-correlation analysis (Zhang and Yeh, 1997; Li and Yeh, 1998; Hughson and Yeh, 2000; Mao et al., 2011; Sun et al., 2013) has been carried out to investigate how the pressure head at a given location is affected by K_s at different locations within a hillslope, based on a Taylor series expansion of the flow model (Eq. (1)). Since natural logarithms of saturated hydraulic conductivity, $\ln K_s$, at different locations within the hillslope are treated as a random field with some spatial correlation, we express them as $\ln K_s = F = \overline{F} + f$, where f represents the spatial variability or uncertainty due to

lack of measurements of K_s or $\ln K_s$. Likewise, the pressure head is represented by $P = \overline{P} + p$, where $\overline{P}$ represents the mean pressure head within an equivalent homogeneous hillslope, evaluated using $\overline{F}$, and p denotes the perturbation of pressure head. Subsequently, the pressure head can be expanded in a Taylor series regarding $\overline{F}$:

$$P(x_i, z_i) = \overline{P}(x_i, z_i) + p(x_i, z_i) = \overline{P}(x_i, z_i) +$$
$$\left. \frac{\partial P(x_i, z_i)}{\partial F(x_j, z_j)} \right|_{\overline{F}} f(x_j, z_j) + \frac{1}{2!} \left. \frac{\partial^2 P(x_i, z_i)}{\partial F^2(x_j, z_j)} \right|_{\overline{F}} f^2(x_j, z_j) + \cdots$$
(6)

The partial derivative $\left. \frac{\partial P(x_i, z_i)}{\partial F(x_j, z_j)} \right|_{\overline{F}}$ in Eq. (6) denotes the

sensitivity of P at the location (x_i, z_i) with respect to the perturbation of $\ln K_s$ at the location (x_j, z_j), i.e., $f(x_j, z_j)$. The subscript j ranges from 1 to M, where M is the total number of elements in a finite element mesh for the hillslope. The subscript i ranges from 1 to N, where N is the total number of nodes in the finite element mesh for the hillslope. The repeated subscript j in the product of the sensitivity term and the perturbation term (i.e., f) implies the summation of all products with j, ranging from 1 to M, for the pressure head at node i. After neglecting the second-order and higher-order terms, the first-order approximation of the pressure head perturbation can be written as

$$p(x_i, z_i) \approx \left. \frac{\partial P(x_i, z_i)}{\partial F(x_j, z_j)} \right|_{\overline{F}} f(x_j, z_j)$$
(7)

To reduce the computational load, the sensitivity was calculated with a numerical adjoint state method (Sykes et al., 1985; Li and Yeh, 1998, 1999; Hughson and Yeh, 2000) in this study.

Multiplying Eq. (7) with itself, and based on the following expectation:

$$E[p(x_i, z_i)p(x_k, z_k)] = E\left\{ \left. \frac{\partial P(x_i, z_i)}{\partial F(x_j, z_j)} \right|_{\overline{F}} f(x_j, z_j)f(x_l, z_l) \left. \frac{\partial P(x_k, z_k)}{\partial F(x_l, z_l)} \right|_{\overline{F}} \right\} =$$
$$\left. \frac{\partial P(x_i, z_i)}{\partial F(x_j, z_j)} \right|_{\overline{F}} E[f(x_j, z_j)f(x_l, z_l)] \left. \frac{\partial P(x_k, z_k)}{\partial F(x_l, z_l)} \right|_{\overline{F}}$$
(8)

where $i, k = 1, 2, \cdots, N$, and $j, l = 1, 2, \cdots, M$, we generate the following relation:

$$t[R_{pp}(x_i, z_i; x_k, z_k)] = \left[\left. \frac{\partial P(x_i, z_i)}{\partial F(x_j, z_j)} \right|_{\overline{F}} \right] [R_{ff}(x_j, z_j; x_l, z_l)] \cdot$$
$$\left[\left. \frac{\partial P(x_k, z_k)}{\partial F(x_l, z_l)} \right|_{\overline{F}} \right]^{\mathrm{T}}$$
(9)

where $[R_{pp}]$ is the $N \times N$ covariance matrix for P, $[R_{ff}]$ is the $M \times M$ covariance matrix for $\ln K_s$, and $\left[\left. \frac{\partial P(x_i, z_i)}{\partial F(x_j, z_j)} \right|_{\overline{F}} \right]$ and $\left[\left. \frac{\partial P(x_k, z_k)}{\partial F(x_l, z_l)} \right|_{\overline{F}} \right]$ are $N \times M$ matrices. Each diagonal element of

$[R_{pp}]$ is the pressure head variance σ_p^2 at the location (x_i, z_i), representing the mean-square deviation of the pressure head within a heterogeneous hillslope from the mean pressure head $\overline{P}$, calculated using the $\overline{F}$ value of the hillslope.

Similarly, multiplying Eq. (7) with $f(x_l, z_l)$ and with the following expectation:

$$E[p(x_i, z_i)f(x_l, z_l)] = E\left[\left. \frac{\partial P(x_i, z_i)}{\partial F(x_j, z_j)} \right|_{\overline{F}} f(x_j, z_j)f(x_l, z_l) \right] =$$
$$\left. \frac{\partial P(x_i, z_i)}{\partial F(x_j, z_j)} \right|_{\overline{F}} E[f(x_j, z_j)f(x_l, z_l)]$$
(10)

we obtain the cross-covariance between the pressure head P at the location (x_i, z_i) and $\ln K_s$ at the location (x_l, z_l):

$$[R_{pf}(x_i, z_i; x_l, z_l)] = \left[\left. \frac{\partial P(x_i, z_i)}{\partial F(x_j, z_j)} \right|_{\overline{F}} \right] [R_{ff}(x_j, z_j; x_l, z_l)]$$
(11)

where $[R_{pf}]$ represents the cross-covariance function matrix between the pressure head P and $\ln K_s$.

R_{pf} is normalized by the square root of the product of $\sigma_p^2(x_i, z_i)$ and $\sigma_f^2(x_l, z_l)$ to obtain the corresponding cross-correlation ρ_{pf}:

$$[\rho_{pf}(x_i, z_i; x_l, z_l)] = \frac{[R_{pf}(x_i, z_i; x_l, z_l)]}{\sqrt{\sigma_p^2(x_i, z_i)\sigma_f^2(x_l, z_l)}} = \frac{\left[\left. \frac{\partial P(x_i, z_i)}{\partial F(x_j, z_j)} \right|_{\overline{F}} \right] [R_{ff}(x_j, z_j; x_l, z_l)]}{\sqrt{\sigma_p^2(x_i, z_i)\sigma_f^2(x_l, z_l)}}$$
(12)

where $[\rho_{pf}]$ is the cross-correlation function matrix between the pressure head P and $\ln K_s$.

Here we must point out that this cross-correlation analysis is based on the first-order approximation, which ignores the higher-order terms in the Taylor series. As a computationally efficient approach, this cross-correlation analysis has been widely used in inverse modeling as well as joint inversion of flow, solute transport, and geophysical surveys.

2.5. Procedure to select corresponding realization for given hydraulic scenario

There are an infinite number of realizations of K_s fields of a heterogeneous hillslope with the same prescribed statistical parameters. When a certain hydraulic scenario, for example, the pressure head at the hillslope toe reaching its maximum, is selected, few realizations may exist whose hydraulic responses satisfy this hydraulic scenario. To select these possible realizations, we take advantage of the preceding cross-correlation analysis.

According to Eq. (7), we know that the pressure head P at one location is influenced by K_s or $\ln K_s$ at different locations within a hillslope. The cross-correlation $\rho_{pf} > 0$ means that

an increase in K_s or $\ln K_s$ at the location (x_j, z_j) can lead to an increase in the pressure head P at the selected location (x_i, z_i) within the hillslope and vice versa (positively-correlated), while $\rho_{pf} < 0$ means that an increase in K_s or $\ln K_s$ at the location (x_j, z_j) produces a decrease in the pressure head P at the selected location (x_i, z_i) and vice versa (negatively-correlated), and $\rho_{pf} = 0$ means no connection between K_s or $\ln K_s$ and the pressure head P. That is, the cross-correlation ρ_{pf} could be considered normalized weights, which quantify the influences of K_s or $\ln K_s$ at different locations on the pressure head P at some selected crucial locations within the hillslope.

Accordingly, a criterion A_e is set up to select the realization that best meets the requirement of a hydraulic scenario:

$$A_e = \sum_{i \in (1, N)} \sum_{j=1}^{M} \rho_{pf} \ln K_s(x_j, z_j) \tag{13}$$

or

$$A_e = \sum_{i \in (1, N)} \sum_{j=1}^{M} \rho_{pf} K_s(x_j, z_j) \tag{14}$$

where $e = 1, 2, \cdots, L$, which denotes the numbers of generated realizations of K_s fields of the hillslope. $i \in (1, N)$ means that the selected crucial locations for the pressure heads could be a point group or just one point. For each realization of the K_s field within the hillslope, A_e could be calculated with Eq. (13) or Eq. (14). The maximum of A_e indicates that the pressure head at the selected location reaches a maximum, and the minimum of A_e indicates that the pressure head at the selected location reaches a minimum. That is to say, A_e can be used as the criterion for selection of a realization, which satisfies the given hydraulic scenario, from an infinite number of realizations with the same prescribed statistical parameters.

In fact, there may exist other possible realizations that satisfy the given hydraulic scenario, and the selected realization may not be unique. Here we merely use this procedure to select some realizations for illustration purposes. That is, we want to demonstrate what the likely distributions of saturated hydraulic conductivity and flow field within a heterogeneous hillslope might look like for some given critical hydraulic scenarios, with different rainfall amounts and spatial statistics, which describe the heterogeneous nature of saturated hydraulic conductivity within the hillslope.

3. Setup of simulations

3.1. Model and parameters

In order to investigate the relation between the most likely distribution of saturated hydraulic conductivity and the observed pressure head distribution within a hillslope, several numerical experiments were conducted. All the experiments were based on a synthetic 2D vertical cross-section of a hypothetical hillslope. Fig. 1 displays the geometry and boundary conditions of the hillslope. The boundaries AH and

BC are the Dirichlet boundaries with constant heads, that is, $(P + z)|_{AH} = 20$ m, and $(P + z)|_{BC} = 10$ m. The boundary AB is impermeable, and the boundary GF is the Neumann boundary with a constant vertical flux q. The boundaries FE, ED, GH, and DC are defined as seepage faces. The boundaries FE and ED vary from the Neumann boundaries with constant q in the unsaturated state to boundaries with zero pressure head in the saturated state. The boundaries GH and DC vary from impermeable boundaries in the unsaturated state to boundaries with zero pressure head in the saturated state. The simulation domain (100 m × 40 m) in the vertical plane is evenly discretized into 50 × 40 elements and 2091 nodes, and then the top right corner of the domain is truncated. Thus, the shape of the remaining part with 1610 elements and 1681 nodes becomes the geometry of the hillslope (Fig. 1).

Stochastic representation of the heterogeneous hillslope (as discussed in the preceding section) was used to provide a quantitative but bulk description of the heterogeneity within the hillslope. μ_{K_s} was set to 1.0 m/d. The values of soil hydraulic parameters, set to be uniform in this study, were as follows: $\alpha = 0.4$ m^{-1}, $m = 0.5$, $n = 2$, $\theta_r = 0.07$, and $\theta_s = 0.4$. Table 1 lists the spatial statistics of K_s used in the numerical experiments. In this study, only K_s was treated as a random field, although other parameters also exhibited spatial variability. These statistical values were selected based on comprehensive surveys of literature on spatial variability of unsaturated hydraulic parameters, as summarized in Yeh et al. (2015). Based on published studies (Nielsen et al., 1973; Rawls et al., 1982; Carsel and Parrish, 1988; Ünlü et al., 1990; White and Sully, 1992; Russo and Bouton, 1992; Khaleel and Freeman, 1995; Russo, 1997; Gui et al., 2000; Srivastava et al., 2010; Santoso et al., 2011; Cho, 2012; Zhu et al., 2013), a general range of 30%−100% of the coefficient of variation ($CV = \sigma_{K_s}/\mu_{K_s}$) of K_s was suggested. Thus, the general range of variance of $\ln K_s$ could be 0.1 to 0.7, and we also used a high variance of 1.5 for comparison. Correlation scales of 0.025−100 times the slope height were suggested for $\ln K_s$, which were 0.5−2000 m in Zhu et al. (2013). Actually, not only the slope height, but also the grid size and entire domain size needed to be considered to determine a
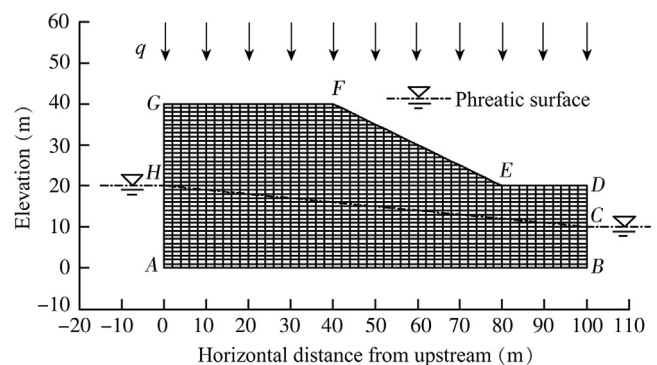

Fig. 1. Hypothetical hillslope in numerical study.

Table 1
Study cases.

Case no.	σ_f^2	λ_h (m)	λ_v (m)	λ_h/λ_v	q/μ_{K_s}
1	0.7	10	10	1	0.01
2	1.5	10	10	1	0.01
3	0.7	50	10	5	0.01
4	0.7	100	10	10	0.01
5	0.7	10	10	1	0.03
6	0.7	10	10	1	0.05

Fig. 2. Mean pressure head evaluation for homogeneous hillslope when $K_s = \mu_{K_s} = 1.0$ m/d.

proper correlation scale. Meanwhile, the anisotropy of $\ln K_s$ could not be neglected. In this study, the correlation scale of $\ln K_s$ in the vertical direction, λ_v, was determined to be 10 m, and the correlation scale of $\ln K_s$ in the horizontal direction, λ_h, was changed from 10 to 100 m. The ratio between the vertical infiltration flux q and μ_{K_s} was set to 0.01 (mild rainfall intensity) based on Zhu et al. (2013), and we increased this value to 0.05 for comparison purposes. These small values are shown to be able to maintain a constant matric suction in the unsaturated region (Zhang et al., 2004), and make the constant infiltration flux boundary realistic.

In the analysis, the six cases listed in Table 1 were used in parametric studies on the effect of three factors, which were the variance (σ_f^2), spatial structure anisotropy (λ_h/λ_v), and normalized vertical infiltration flux (q/μ_{K_s}). More specifically, cases 1 and 2 focused on the effects of the variation of σ_f^2; cases 1, 3, and 4 focused on the effects of the variation of λ_h/λ_v; and cases 1, 5, and 6 focused on the effects of the variation of q/μ_{K_s}.

A finite element numerical model code for simulating variably saturated flow and transport in two dimensions (VSAFT2), presented by Yeh et al. (1993), with the corresponding software available at www.hwr.arizona.edu/yeh, was used to simulate flow fields for the hillslope scenario. This program solves Eq. (1) with nonlinear finite element approximation based on the Newton-Raphson method. The program also includes an iterative scheme, since it needs to arrive at the appropriate boundary condition along seepage faces (Rulon and Freeze, 1985).

3.2. Flow field within a homogeneous hillslope

To present a basic understanding of the flow field within the hypothetical hillslope, we first simulated the steady flow in the hillslope, in which the K_s values of all elements were assumed to be the mean saturated hydraulic conductivity (i.e., $\mu_{K_s} = 1.0$ m/d), other parameters were assumed to be uniform, and the vertical infiltration flux was $q = 0.01$ m/d. Fig. 2 shows the simulated flow field, including streamlines (or flow lines), contour lines of pressure head, and the phreatic surface. The flow field derived from the homogeneous mean parameter values represents the most likely flow field with given infiltration rates and boundary conditions. Although this most likely field can be quite different from the field based on heterogeneous parameters, it displays the general flow field within the hillslope.
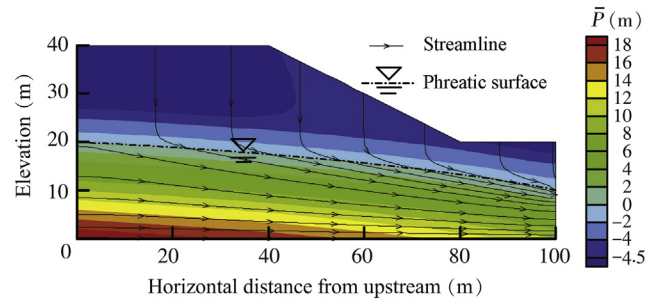
4. Results and discussion

4.1. Cross-correlation analysis

First, we used cross-correlation analysis to investigate how the pressure head at a location is affected by K_s or $\ln K_s$ at different locations within the hypothetical hillslope in case 1. As shown in Fig. 3(a), the spatial distribution of cross-correlation between $\ln K_s$ at different locations and P with the observation location at the slope toe is used to represent the situation in the unsaturated region, while the spatial distribution of cross-correlation with the observation location of P under the slope toe, below the mean position of the phreatic surface, as shown in Fig. 3(b), is representative of the situation in the saturated region. Fig. 3 indicates that the distribution of cross-correlation for the pressure head observation location in the unsaturated region is quite different from that for the pressure head observation
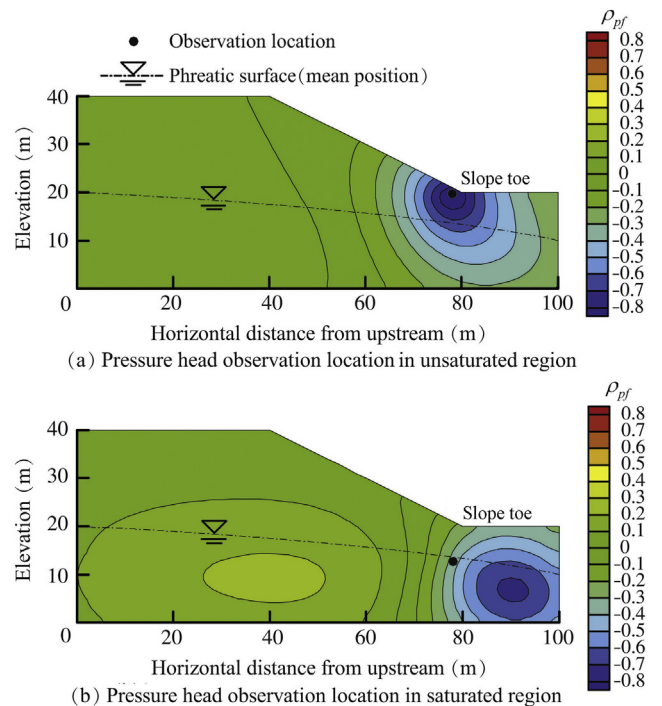

(a) Pressure head observation location in unsaturated region

(b) Pressure head observation location in saturated region

Fig. 3. Spatial distributions of cross-correlation between $\ln K_s$ and P in steady state for case 1.

location in the saturated region; however, the distributions of cross-correlation have similar characteristics in the unsaturated region and saturated region, respectively, regardless of the pressure head observation location.

As illustrated in Fig. 3(a), in the unsaturated region, the pressure head is negatively correlated with $\ln K_s$ in the region around the pressure head observation location at the slope toe, with a cross-correlation value reaching −0.8. As the distance from the pressure head observation location (e.g., the slope toe) increases, the cross-correlation values tend to be less negative, showing a decreasing correlation, and finally become slightly positive in the upstream region. Overall, the pressure head at the slope toe is dominated by negative cross-correlation with $\ln K_s$. These results also demonstrate that the pressure head at an observation location within the hillslope is not equally influenced by heterogeneity everywhere within the hillslope, and the most influenced region is around the pressure head observation location at the slope toe, as shown in Fig. 3(a).

As shown in Fig. 3(b), in the saturated region, the pressure head at the observation location is positively correlated with $\ln K_s$ in the upstream region and negatively correlated with $\ln K_s$ in the downstream region. This pattern of correlation follows the direction of the streamline (see Fig. 2 for the streamline). This result is consistent with the findings in Li and Yeh (1999) and Mao et al. (2011). Specifically, the pressure head is positively correlated with K_s in the up-gradient region and negatively correlated with K_s in the down-gradient region with respect to the pressure head observation location along the streamline toward the pumping well. Here, the drain outlet of the downstream slope is equivalent to a pumping well. Yeh et al. (2014) used a simple example to elucidate this relationship.

4.2. Effect of three factors on results of cross-correlation analysis

For cases 1 through 6 in Table 1, cross-correlation analysis was used to investigate the degree of influence of $\ln K_s$ at different locations within the hillslope on the pressure head with the observation location at the slope toe in the steady state. The resultant spatial distributions of cross-correlation within the hillslope for the six cases are shown in Fig. 4. Note that σ_f^2, λ_h/λ_v, and q/μ_{K_s} have similar effects when the pressure head observation location is in the saturated region.

Comparison of case 1 and case 2 in Fig. 4 indicates that σ_f^2 has no effect on the spatial distribution of cross-correlation between $\ln K_s$ and P. This is due to the fact that the cross-correlation value is obtained by normalizing the cross-covariance R_{pf} using the square root of the product of σ_p^2 and σ_f^2.

When we compare case 1, case 3, and case 4, we find that, with the increase of spatial structure anisotropy, λ_h/λ_v, the pattern of spatial distribution of cross-correlation becomes more stratified. When the observation location of pressure head is in the unsaturated region, the negatively correlated region increases with the value of λ_h/λ_v, and the cross-correlation value between $\ln K_s$ and P of the whole region

within the hillslope becomes more negative. The positively correlated region, formerly existing in the upstream region, is gradually covered by the negatively correlated region with the increase of λ_h/λ_v. The reason for these phenomena is that, with the increasing spatial structure anisotropy of K_s, the autocorrelation between K_s at any two locations increases, leading to the increase of the negatively correlated region.

Comparisons of case 1, case 5, and case 6 demonstrate that an increase in the vertical infiltration flux q changes the spatial distribution of cross-correlation between $\ln K_s$ and P. More specifically, the negatively correlated region increases with the value of q, and the most negative value of cross-correlation becomes less negative. This result can be attributed to the fact that the flow fields are different for different vertical infiltration fluxes. However, this change is not very dramatic.

4.3. Spatial distribution pattern of saturated hydraulic conductivity with respect to pressure head within a heterogeneous hillslope

Based on the spatial distributions of cross-correlation in Figs. 3(a) and 4, we can further conclude that, in the unsaturated region, subject to a constant flux (or Neumann) boundary, the location with a relatively high P is in a relatively low K_s zone, while the location with a relatively low P is in a relatively high K_s zone. This can be attributed to the fact that, in the unsaturated region, the dominant correlation between P and K_s is negative and mainly occurs around the pressure head observation location. The matric suction (i.e., the absolute value of negative pore-water pressure) in a relatively low K_s zone is low, and there may even exist high positive pressures. Therefore, the relatively low K_s zones in the unsaturated region close to the slope surface are the more likely deformation and failure zones, which require special attention and prevention.

On the other hand, based on Fig. 3(b), we can determine that, in the saturated region subject to a constant pressure head (or Dirichlet) boundary, if a location has a relatively high P or is under a relatively high phreatic surface, the upstream region is a relatively high K_s zone while the downstream region is a relatively low K_s zone. Meanwhile, if the P value or the phreatic surface is relatively low at a location, a relatively high K_s zone exists downstream, while a relatively low K_s zone exists upstream.

Note that this spatial distribution pattern of K_s is valid only for the boundary conditions considered here. For example, if we assign a constant head (or Dirichlet) boundary along *GF*, *FE*, or *ED* (Fig. 1) in the unsaturated region (e.g., pond and surface water), then the pattern in the unsaturated region will be similar to that in the saturated region. As a result, the pattern depends on the boundary condition.

4.4. Examples of realizations for given hydraulic scenarios

Using the procedure to select realizations for given hydraulic scenarios (Eq. (13) or (14)), realizations of K_s fields and the corresponding flow fields for the six cases that satisfy

Fig. 4. Spatial distributions of cross-correlation between lnK_s at different locations and P at slope toe in steady state for different cases.

the hydraulic scenarios, in which the pressure head at the slope toe reaches a maximum or minimum, were obtained. Ten thousand realizations were generated for each case. We must emphasize that here the hydraulic scenario focused on just the slope toe, the only observation location within the hillslope. If the target changes or expands, the selected realizations will change.

4.4.1. Pressure head at slope toe reaching maximum

Fig. 5 shows the selected K_s random fields and their corresponding flow fields, conditioned to the scenario in which the pressure head at the slope toe is maximum. As illustrated in Fig. 5, the selected realizations for the six different cases all have high K_s values in the upstream region and low K_s values in the downstream region, and the slope toe is located in a relatively low K_s zone. In the unsaturated region, a relatively low P value tends to exist in a relatively high K_s zone. Such spatial distributions of K_s are consistent with the cross-correlation pattern between K_s and P, and correspond to the

maximum pressure head at the slope toe under the prescribed boundary conditions.

In addition, for case 1, shown in Fig. 5(a), the K_s field fluctuates spatially, each high/low K_s zone is surrounded by other low/high K_s zones, and there appears to be no preferential distribution direction. This is reasonable in realistic conditions when this slope soil profile is within regionally similar deposits without a specific depositional direction. Case 2 shows the spatial distribution of K_s similar to that in case 1, but with a greater difference between the high K_s value and the low K_s value within the hillslope (i.e., greater heterogeneity). The spatial distributions of K_s in cases 3 and 4 are horizontally stratified, representing a horizontally layered slope, although in case 3 there exist some small discontinuities (e.g., high K_s zone-like fractures and low K_s zone-like barriers) in each layer. The spatial distributions of K_s in cases 5 and 6 are similar to that in case 1, since their cross-correlation patterns are similar, as illustrated in the preceding section (Figs. 4(a), (e), and (f)).
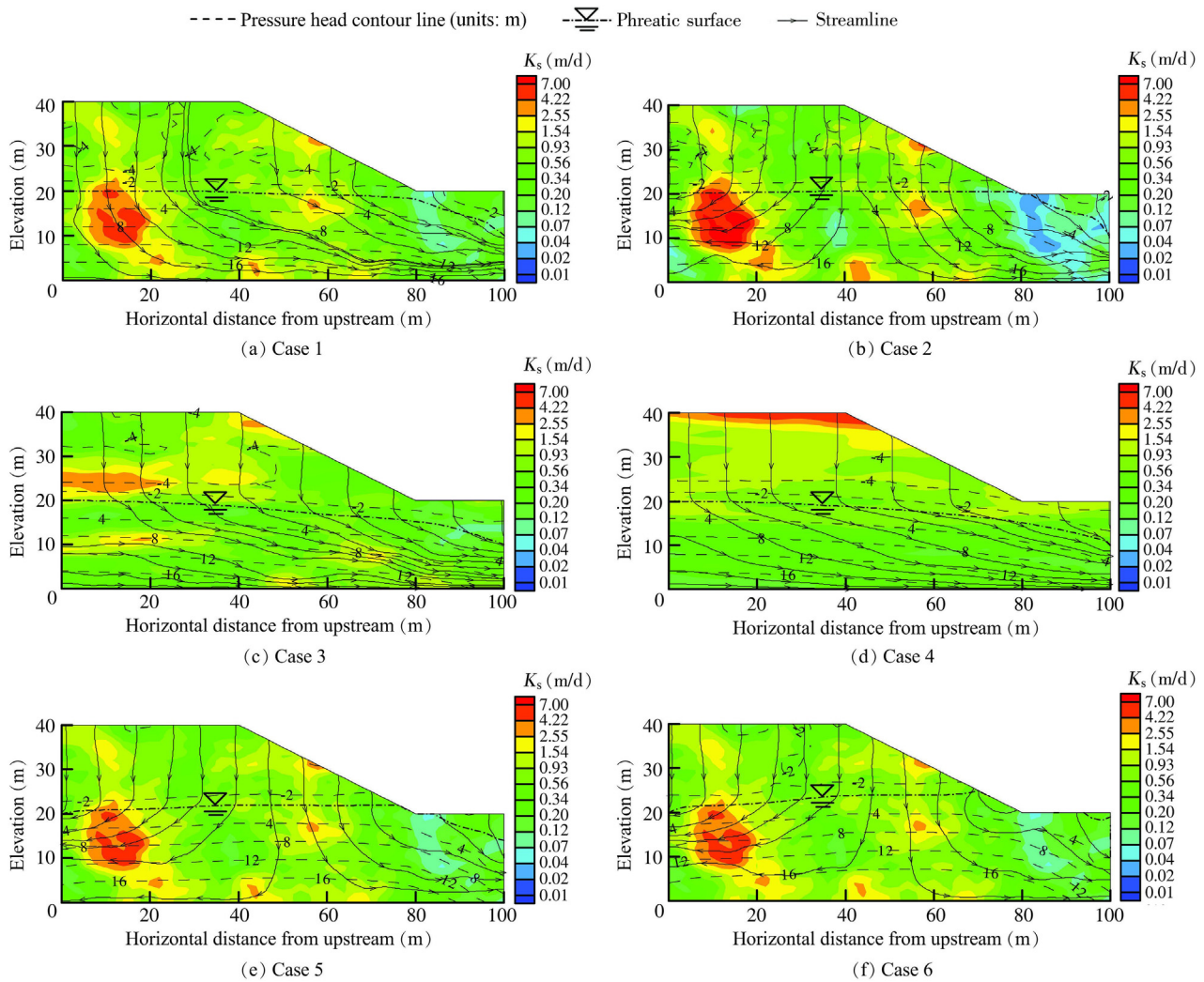
Fig. 5. Spatial distributions of realized K_s fields and flow fields in steady state for different cases, subject to hydraulic scenario in which pressure head at slope toe reaches a maximum.

Comparing case 1 with case 2 in Fig. 5, we find that a higher σ_f^2 leads to a greater difference between the high K_s value and the low K_s value within the hillslope. This also results in a higher phreatic surface and a higher pressure head at the slope toe.

Comparisons of case 1, case 3, and case 4 in Fig. 5 demonstrate that when the K_s random field of selected realizations becomes more stratified, the field tends to show smooth variation within the horizontal layers, and the K_s values tend to be low in most regions of the hillslope, especially in the saturated region below the phreatic surface. This leads to a lower phreatic surface and a lower pressure head at the slope toe. Moreover, the corresponding streamlines become straighter and smoother, making them similar to the streamlines in the homogeneous hillslope in Fig. 2. These results suggest that an isotropic hillslope with relatively small correlation scales may produce a small number of patches of high positive pressure in the unsaturated region, which are localized and hard to detect, but may be critical for slope stability analysis. On the other hand, horizontally layered slopes are more likely to produce large-scale hydraulic features (e.g., perched water table aquifers), which are easier to detect.

Comparisons of case 1, case 5, and case 6 in Fig. 5 indicate that an increase in the vertical infiltration flux q produces a higher phreatic surface and a higher pressure head at the slope toe.

4.4.2. Pressure head at slope toe reaching minimum

Fig. 6 shows heterogeneous K_s fields and their corresponding flow fields, subject to the condition that the pressure head at the slope toe must be at a minimum. Each realization for each case in Fig. 6 has similar characteristics of spatial distribution of K_s to that in Fig. 5. However, unlike the realizations in Fig. 5, the selected realizations for six different cases in Fig. 6 all have high K_s values, mainly distributed in the downstream regions, and low K_s values, mainly distributed in the upstream regions, and the slope toe is in a relatively high K_s zone. In the unsaturated region, a relatively high P value tends to exist in a relatively low K_s zone. Moreover, the

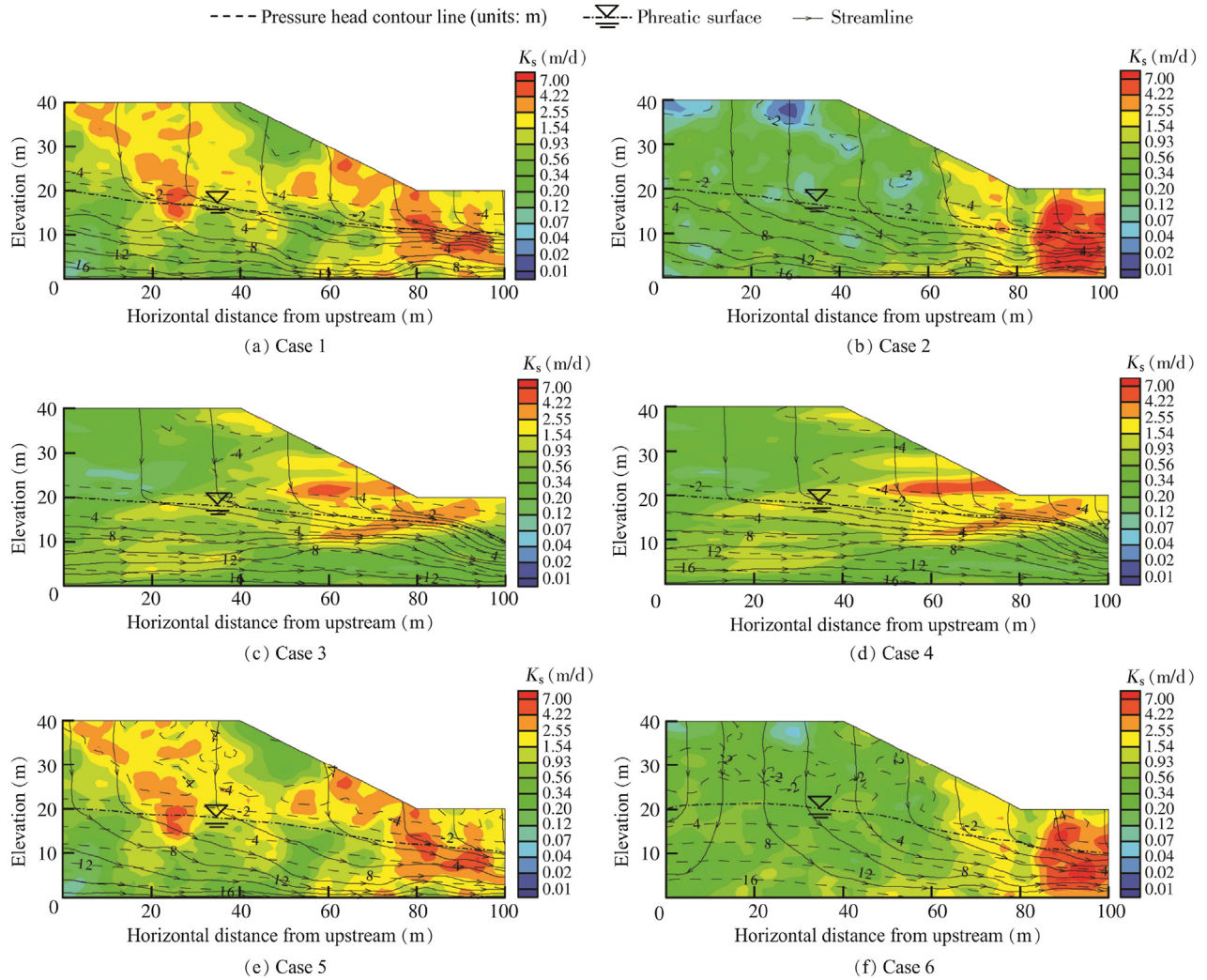- - - - Pressure head contour line (units: m)   ⏢ Phreatic surface   → Streamline

Fig. 6. Spatial distributions of realized K_s fields and flow fields in steady state for different cases, subject to hydraulic scenario in which pressure head at slope toe reaches a minimum.

phreatic surfaces for different cases in Fig. 6 are all lower than those in Fig. 5. Note that even if the vertical infiltration flux increases (e.g., case 6 in Fig. 6), the phreatic surface can still remain low, depending on the distribution of K_s within the heterogeneous hillslope. In addition, the effects of σ_f^2, λ_h/λ_v, and q/μ_{K_s} as shown in Fig. 6 are similar to those in Fig. 5.

5. Conclusions

Results of the study show that, in an unsaturated region with a flux boundary, the dominant correlation between the pressure head P and saturated hydraulic conductivity K_s is negative and mainly occurs around the observation location of P. A location with a relatively high P is in a relatively low K_s zone, while a location with a relatively low P is in a relatively high K_s zone. The relatively low K_s zones in the unsaturated region close to the slope surface are the more likely deformation and failure zones, which deserve special attention. We can further define the ratio of the vertical infiltration flux q to K_s (i.e., q/K_s), with the vertical infiltration flux q set to be

constant and uniform in this study. Therefore, P was positively correlated with q/K_s at the same location in the unsaturated region. Note that rainfall distribution is also important to the spatial distribution of P in unsaturated regions. If rainfall is non-uniform, the correlation between P and K_s becomes more complex. However, P is still positively correlated with q/K_s. In addition, the position and shape of the phreatic surface may reveal the spatial distribution of K_s in a saturated region. That is, even if the vertical infiltration flux increases, the phreatic surface can remain low, depending on the distribution of K_s within the heterogeneous hillslope.

The most likely spatial pattern of the K_s field depends on the applied boundary conditions and factors, like the variance of $\ln K_s$, spatial structure anisotropy of $\ln K_s$, and vertical infiltration flux q. Overall, the spatial pattern obtained in this study can serve as a useful tool to quickly grasp the most likely distribution pattern of K_s within a hillslope using observed pressure head fluctuations. Based on these findings, we conclude that, in terms of hillslope stability, heterogeneity causes some parts of the hillslope to be sensitive to external

hydraulic stimuli (e.g., rainfall and reservoir level change) and other parts of the hillslope to be insensitive. This is due to the fact that heterogeneity affects the spatial distributions of the matric suction (i.e., the absolute value of negative pore-water pressure), pressure head, and position and shape of the phreatic surface. This finding is essential since it explains why slopes with similar geometries would have different hydraulic or deformation responses to the same hydraulic stimuli. For example, some hillslopes are rainfall-sensitive while others are rainfall-insensitive in terms of hillslope stability. Research on these topics for hillslope stability analysis will be reported in future papers.

References

Bouwer, H., 1978. Groundwater Hydrology. McGraw-Hill College, New York.

Carsel, R.F., Parrish, R.S., 1988. Developing joint probability distributions of soil water retention characteristics. Water Resour. Res. 24(5), 755−769. http://dx.doi.org/10.1029/WR024i005p00755.

Cho, S.E., 2012. Probabilistic analysis of seepage that considers the spatial variability of permeability for an embankment on soil foundation. Eng. Geol. 133−134, 30−39. http://dx.doi.org/10.1016/j.enggeo.2012.02.013.

Cho, S.E., 2014. Probabilistic stability analysis of rainfall-induced landslides considering spatial variability of permeability. Eng. Geol. 171, 11−20. http://dx.doi.org/10.1016/j.enggeo.2013.12.015.

Fenton, G.A., Griffiths, D.V., 1993. Statistics of block conductivity through a simple bounded stochastic medium. Water Resour. Res. 29(6), 1825−1830. http://dx.doi.org/10.1029/93WR00412.

Gelhar, L.W., 1993. Stochastic Subsurface Hydrology. Prentice-Hall, Englewood Cliffs.

Griffiths, D.V., Fenton, G.A., 1993. Seepage beneath water retaining structures founded on spatially random soil. Géotechnique 43(4), 577−587. http://dx.doi.org/10.1680/geot.1993.43.4.577.

Griffiths, D.V., Fenton, G.A., 2004. Probabilistic slope stability analysis by finite elements. J. Geotech. Geoenvironmental Eng. 130(5), 507−518. http://dx.doi.org/10.1061/(ASCE)1090-0241(2004)130:5(507).

Gui, S., Zhang, R., Turner, J.P., Xue, X., 2000. Probabilistic slope stability analysis with stochastic soil hydraulic conductivity. J. Geotech. Geoenvironmental Eng. 126(1), 1−9. http://dx.doi.org/10.1061/(ASCE)1090-0241(2000)126:1(1).

Gutjahr, A.L., 1989. Fast Fourier Transforms for Random Field Generation: Project Report for Los Alamos Grant to New Mexico Tech. New Mexico Institute of Mining and Technology, Socorro.

Hughson, D.L., Yeh, T.C.J., 2000. An inverse model for three-dimensional flow in variably saturated porous media. Water Resour. Res. 36(4), 829−839. http://dx.doi.org/10.1029/2000WR900001.

Khaleel, R., Freeman, E.J., 1995. Variability and Scaling of Hydraulic Properties for 200 Area Soils, Hanford Site. Westinghouse Hanford Company, Richland.

Li, B., Yeh, T.C.J., 1998. Sensitivity and moment analyses of head in variably saturated regimes. Adv. Water Resour. 21(6), 477−485. http://dx.doi.org/10.1016/S0309-1708(97)00011-0.

Li, B., Yeh, T.C.J., 1999. Cokriging estimation of the conductivity field under variably saturated flow conditions. Water Resour. Res. 35(12), 3663−3674. http://dx.doi.org/10.1029/1999WR900268.

Mao, D., Wan, L., Yeh, T.C.J., Lee, C., Hsu, K., Wen, J., Lu, W., 2011. A revisit of drawdown behavior during pumping in unconfined aquifers. Water Resour. Res. 47(5). http://dx.doi.org/10.1029/2010WR009326.

Mualem, Y., 1976. A new model for predicting the hydraulic conductivity of unsaturated porous media. Water Resour. Res. 12(3), 513−522. http://dx.doi.org/10.1029/WR012i003p00513.

Nielsen, D.R., Biggar, J.W., Erh, K.T., 1973. Spatial variability of field-measured soil-water properties. Hilgardia 42(7), 215−259. http://dx.doi.org/10.3733/hilg.v42n07p215.

Rawls, W.J., Brakensiek, D.L., Saxtonn, K.E., 1982. Estimation of soil water properties. Trans. ASAE 25(5), 1316−1320. http://dx.doi.org/10.13031/2013.33720.

Rulon, J.J., Freeze, R.A., 1985. Multiple seepage faces on layered slopes and their implications for slope-stability analysis. Can. Geotech. J. 22(3), 347−356. http://dx.doi.org/10.1139/t85-047.

Russo, D., Bouton, M., 1992. Statistical analysis of spatial variability in unsaturated flow parameters. Water Resour. Res. 28(7), 1911−1925. http://dx.doi.org/10.1029/92WR00669.

Russo, D., 1997. On the estimation of parameters of log-unsaturated conductivity covariance from solute transport data. Adv. Water Resour. 20(4), 191−205. http://dx.doi.org/10.1016/S0309-1708(96)00019-X.

Santoso, A.M., Phoon, K.K., Quek, S.T., 2011. Effects of soil spatial variability on rainfall-induced landslides. Comput. Struct. 89(11), 893−900. http://dx.doi.org/10.1016/j.compstruc.2011.02.016.

Srivastava, A., Babu, G.L.S., Haldar, S., 2010. Influence of spatial variability of permeability property on steady state seepage flow and slope stability analysis. Eng. Geol. 110(3), 93−101. http://dx.doi.org/10.1016/j.enggeo.2009.11.006.

Sun, R., Yeh, T.C.J., Mao, D., Jin, M., Lu, W., Hao, Y., 2013. A temporal sampling strategy for hydraulic tomography analysis. Water Resour. Res. 49(7), 3881−3896. http://dx.doi.org/10.1002/wrcr.20337.

Sykes, J.F., Wilson, J.L., Andrews, R.W., 1985. Sensitivity analysis for steady state groundwater flow using adjoint operators. Water Resour. Res. 21(3), 359−371. http://dx.doi.org/10.1029/WR021i003p00359.

Ünlü, K., Nielsen, D.R., Biggar, J.W., Morkoc, F., 1990. Statistical parameters characterizing the spatial variability of selected soil hydraulic properties. Soil Sci. Soc. Am. J. 54(6), 1537−1547. http://dx.doi.org/10.2136/sssaj1990.03615995005400060005x.

van Genuchten, M.T., 1980. A closed-form equation for predicting the hydraulic conductivity of unsaturated soils. Soil Sci. Soc. Am. J. 44(5), 892−898. http://dx.doi.org/10.2136/sssaj1980.03615995004400050002x.

White, I., Sully, M.J., 1992. On the variability and use of the hydraulic conductivity alpha parameter in stochastic treatments of unsaturated flow. Water Resour. Res. 28(1), 209−213. http://dx.doi.org/10.1029/91WR02198.

Wu, C., Yeh, T.C.J., Zhu, J., Lee, T.H., Hsu, N., Chen, C., Sancho, A.F., 2005. Traditional analysis of aquifer tests: Comparing apples to oranges? Water Resour. Res. 41(9), W09402. http://dx.doi.org/10.1029/2004WR003717.

Yeh, T.C.J., 1992. Stochastic modelling of groundwater flow and solute transport in aquifers. Hydrol. Process 6(4), 369−395. http://dx.doi.org/10.1002/hyp.3360060402.

Yeh, T.C.J., Srivastava, R., Guzman, A., Harter, T., 1993. A numerical model for water flow and chemical transport in variably saturated porous media. Groundwater 31(4), 634−644. http://dx.doi.org/10.1111/j.1745-6584.1993.tb00597.x.

Yeh, T.C.J., Mao, D., Zha, Y., Hsu, K., Lee, C., Wen, J., Lu, W., Yang, J., 2014. Why hydraulic tomography works? Groundwater 52(2), 168−172. http://dx.doi.org/10.1111/gwat.12129.

Yeh, T.C.J., Khaleel, R., Carroll, K.C., 2015. Flow Through Heterogeneous Geological Media. Cambridge University Press, Cambridge.

Zhang, J., Yeh, T.C.J., 1997. An iterative geostatistical inverse method for steady flow in the vadose zone. Water Resour. Res. 33(1), 63−71. http://dx.doi.org/10.1029/96WR02589.

Zhang, L.L., Fredlund, D.G., Zhang, L.M., Tang, W.H., 2004. Numerical study of soil conditions under which can be maintained. Can. Geotech. J. 41(4), 569−582. http://dx.doi.org/10.1139/t04-006.

Zhu, H., Zhang, L.M., Zhang, L.L., Zhou, C.B., 2013. Two-dimensional probabilistic infiltration analysis with a spatially varying permeability function. Comput. Geotech. 48, 249−259. http://dx.doi.org/10.1016/j.compgeo.2012.07.010.